Supporting Information

Dynamic Pyridinethiol Ligand Shuttling within Iron-Anchored Covalent Organic Frameworks Boosts CO_2 Photoreduction

Yong-Kang Zhang,[a] *Lan Zhao,*[a] *Alexander O. Terent'ev,*[b] *Liang-Nian He**[a]

[a] State Key Laboratory and Institute of Elemento-Organic Chemistry, Frontiers Science Center for New Organic Matter, College of Chemistry, Nankai University, Tianjin 300071, P. R. China

[b] Zelinsky Institute of Organic Chemistry, Russian Academy of Sciences, 47 Leninsky Prospect, Moscow 119991, Russia

*Corresponding Author
E-mail Addresses: heln@nankai.edu.cn (L.-N. He)

Table of Contents

1. Materials

All the solvents were purchased from Tianjin Bohua Chemical Reagents Co. Ltd. And argon (99.998%) and CO_2 (99.999%) were from Tianjin Haolun. The reagents 2,2'-bipyridyl-5,5'-dialdehyde (bpy-CHO, 97%), 1,3,5-tris-(4-aminophenyl)triazine (TAPT, 95%), iron(II) acetylacetonate ($Fe(acac)_2$, 99%), pyridine-2-thiolate (pySH, 98%), 2-mercapto-5-methylpyridine (CH_3-pySH, 97%), 3-aminopyridine-2-thiol (NH_2-pySH, 97%), 2-mercaptonicotinic acid (COOH-pySH, 97%), 5-Chloropyridine-2-thiol (Cl-pySH, 98%), 6-sulfanylnicotinonitrile (CN-pySH, 96%), 2-mercapto-5-nitropyridine (NO_2-pySH, 98%), 2-mercapto-5-(trifluoromethyl)pyridine (CF_3-pySH, 97%), p-toluenethiol (CH_3-phSH, 98%), 2-mercaptopyridine-N-oxide (NO-pySH, 98%), 2-hydroxypyridine-N-oxide (NO-pyOH, 98%), 4-mercaptopyridine (4-pySH, 97%), 2-hydroxythiophenol (2-phSHOH, 99%), 2,2'-dithiodipyridine (pyS-Spy, 98%), 2,2'-bipyridine (bpy, 99%), iron(III) chloride hexahydrate ($FeCl_3 \cdot 6H_2O$, 98%), sodium methoxide (98%), acetic acid (98%), extra dry acetonitrile (CH_3CN, 99.9%) were commercially available and used without further purification. 1,3-dimethyl-2-phenyl-2,3-dihydro-1*H*-benzo[*d*]imidazole (BIH) was synthesized according to the published procedure.[1]

2. Synthesis

Synthesis of bpy-COF: bpy-COF was synthesized according to the reported procedure[2]. In a 10 mL pressure tube, 1,3,5-tris-(4-aminophenyl) triazine (TAPT) (92 mg, 0.26 mmol) and 2,2-bipyridyl-5,5-dialdehyde (82.7 mg, 0.39 mmol) were dispersed in a mixed solution of mesitylene and 1,4-dioxane (6 mL, v/v 5.1/0.9), and ultrasonically dispersed for 30 min. Then 0.2 mL acetic acid was added to the resulting yellow suspension. After degassing with Ar by three freeze-pump-thaw cycles, the tube was sealed and heated to 120 °C for 3 d. The resulting yellow precipitate was collected by filtration and washed with tetrahydrofuran and acetone repeatedly to remove the residual guest molecules. After drying under vacuum at 105 °C for 12 h, the yellow powder was obtained with a yield of 84%.

Synthesis of Fe-bpy-COF: In a 100 mL flask, bpy-COF (160 mg) was treated with $Fe(acac)_2$ (76 mg, 0.3 mmol) in 30 mL of ethanol. First, the reaction mixture is dispersed by sonication for 30 minutes. Then it was stirred at room temperature for 12 h under Ar. After that, the precipitate was collected by filtration and successively washed with 500 mL of ethanol and dried under vacuum at 105 °C for 12 h, affording 165 mg dull yellow powder Fe-bpy-COF.

Synthesis of FeS-bpy-COF: In a 100 mL flask, Fe-bpy-COF (200 mg) was treated with pyridine-2-thiolate (pySH, 89 mg, 0.8 mmol) and sodium methoxide (54 mg, 1 mmol) in 30 mL of methanol. Then, the reaction mixture is sonicated for 30 min, and stirred at room temperature for 12 h under Ar. The precipitate was collected by filtration and successively washed with methanol and diethyl ether. The filter cake was dried under vacuum overnight to produce 181 mg yellowish-green powder FeS-bpy-COF.

Synthesis of $FebpyCl_3$: $FebpyCl_3$ was synthesized according to the literature.[3] The $FeCl_3 \cdot 6H_2O$ (520 mg, 3.7 mmol) was entirely dissolved in 50 mL of ethanol and then a solution of 2,2'-bipyridine (1000 mg, 3.7 mmol) in 50 mL of ethanol was added dropwise to

the stirred solution of $FeCl_3 \cdot 6H_2O$ at room temperature, resulting in an orange solution. The solution was stirred continuously for 12 h, gradually turning to orange suspension. After that, the orange precipitate was collected via filtration and washed with glacial ethanol (10*3 mL) and diethyl ether (5*3 mL) sequentially. Drying the precipitate under vacuum at room temperature produced a yellow powder and the yield was 75% (879 mg). UV-Vis (acetonitrile), 298 nm (ε = 13710 M^{-1} cm^{-1}), 362 nm (ε = 5440 M^{-1} cm^{-1}). Anal. Found: C, 37.05; H, 2.68; N, 7.99. Calculated for $C_{10}H_8N_2FeCl_3$: C, 37.73; H, 2.53; N, 8.80.

3. Characterization

Power X-ray diffraction (XRD) was performed on a Rigaku SmartLab D/max 2500 VL/PC diffractometer with the X-ray source of Cu Kα radiation (λ = 1.5418 Å) at 40 kV, 150 mA and data were collected with a scan rate of 0.5°/min in the range of 2°-40°. FTIR spectra were recorded on a Bruker Tensor-II spectrophotometer. Solid state ^{13}C NMR spectra were measured by Bruker Avance NEO 400 spectrometer. ^{1}H NMR spectra were collected for liquid product analysis at room temperature on a Bruker Avance III 400 spectrometer. Scanning electron microscopy (SEM) images were obtained from FEI Apreo S LoVac emission electron microscope. Transmission electron microscopy (TEM) images were obtained from FEI Tecnai G2 F20 transmission electron microscope. XPS X-ray photoelectron spectra (XPS) data were collected using a Kratos Analytical Axis Ultra DLD spectrometer equipped with a monochromatic Al Kα X-ray source (1486.6 eV) operated at 100 W. After calibration using the binding energy of 284.0 eV of sp^2-C in the C1s peak, the photoelectron spectroscopy was analyzed. Gas adsorption isotherms were conducted on a micromeritics ASAP 2460 instrument. All the samples were outgassed at 100 °C for 4 h in a vacuum before measurements. N_2 gas adsorption isotherms were measured at -196 °C using a liquid N_2 bath. Surface areas were calculated based on Brunauer-Emmett-Teller (BET) method. CO_2 adsorption and desorption isotherms were measured at 0 °C and 25 °C. The relationship between adsorption pressure and CO_2 adsorption at different temperatures was obtained by fitting the adsorption data with the Freundlich isothermal model. Subsequently, the obtained data were substituted into the Clausius-Clapeyron equation to finally acquire the curve of isosteric adsorption heat as a function of CO_2 adsorption. UV-vis absorption spectra were measured on an Agilent Cary 60 spectrometer for liquid samples. UV-vis diffuse reflectance spectroscopy (UV-vis DRS) was conducted on a Hitachi UH4100 spectrometer for solid powder samples with $BaSO_4$ as the reference. Element analysis test was carried out on a vario EL CUBE elementar. Inductively coupled plasma-optical emission spectrometry (ICP-OES) was carried out on a SpectroBlue IL instrument. Steady-state photoluminescence (PL) spectra and Time-resolved photoluminescence (TRPL) decay spectra were recorded at room temperature on an Edinburgh FS5 spectrophotometer. Femtosecond transient absorption spectroscopy (fs-TAS) measurements were performed on a Helios (Ultrafast systems) spectrometers using a regeneratively amplified femtosecond Ti: sapphire laser system (Legend Elite-1K-HE, frequency, 1 kHz; max pulse energy, ~4 mJ; pulse duration, 25 fs) at room temperature. The pump wavelength is 370 nm. Finally, analyze the data through commercial software (Surface Xplorer, Ultrafast Systems). Electrospray ionization mass spectra (ESI/MS) were obtained on an Agilent 6520 Q-TOF LC/MS spectrometer.

4. Photoelectrochemical measurements

All the electrochemical measurements were conducted in 0.5 M Na_2SO_4 electrolyte solution on a CHI potentiostat/galvanostat (CHI660D, CH Instruments Inc., Shanghai) electrochemical working station *via* a standard three-electrode system. The working electrode is indium-doped tin oxide (ITO) glass plate coated with catalyst slurry, the counter electrode is platinum foil, and Ag/AgCl (saturated KCl) as reference electrode, respectively. Mott-Schottky plots were recorded at different frequencies of 500, 1000, and 1500 Hz. Electrochemical impedance spectroscopy (EIS) was recorded over a 0.1-10000 Hz frequency range. The transient photocurrent responses were recorded over a sampling interval of 20 s using a 300 W Xe lamp equipped with an optical filter ($\lambda \geq 400$ nm). Linear sweep voltammetry (LSV) curves were recorded in the range of 0 ~ -1.1 V and the sweep rate was 10 mV/s in 0.5 M $KHCO_3$ electrolyte solution. Cyclic voltammetry (CV) measurements were performed using a four-neck flask with a 3 mm diameter glassy carbon working electrode, Pt sheet auxiliary electrode, and Ag/AgCl (saturated KCl) reference electrode. Electrochemical experiments conducted in 0.1 M tetrabutylammonium hexafluorophosphate in CH_3CN were performed under CO_2 by bubbling for 5 min. The ferrocene was added to organic phase in the last step of the experiments and recorded to calibrate the consistency of the reference electrode, and the corresponding reduction potentials are reported versus the Fc/Fc^+ couple.

5. Preparation of working electrode

The preparation of the working electrode referred to the previously reported procedure[4]: 2 mg sample was dispersed in 480 μL dimethylformamide containing 20 μL Nafion solution (5%) and ultrasound for 30 min. Subsequently, 100 μL of the mixture was dropped on 1*1 cm^2 ITO and left in the air to dry.

6. Photocatalytic CO_2 reduction experiment

For typical run, a 10 mL Schlenk tube containing 1 mg Fe-bpy-COF, 0.4 mM pySH (0.14 mg, 1.2 μmol), 1.5 M H_2O (81 μL, 4.5 mmol) and 0.025 M BIH (16.8 mg, 75 μmol) in 3 mL CH_3CN solution was degassed with CO_2 for three freeze-pump-thaw cycles before irradiation at 20 ºC with a 300 W Xe lamp equipped with an optical filter ($\lambda \geq 400$ nm). The amount of CO and H_2 produced was analyzed by gas chromatography (GC, FuLi 97902II) with a TCD detector equipped with a packed column TDX-01. The typical volume of injected gas was 1 mL aliquots from the headspace of the reaction cell. Calibration curves were obtained by sampling known amounts of H_2 and CO. Additionally, formate product was quantified by ^1H NMR on a Bruker AV400 spectrometer. A certain amount of the reaction solution was withdrawn, and the insoluble substances were removed by filtration. Then 350 μL was taken out to which 100 μL of acetonitrile-d_3 and 50 μL of 10 mM 1,3,5-trimethoxybenzene (TMB) in CH_3CN as internal standard were added. A calibration curve for the detection of formate was determined from the ratio between the area of the formate C-H peak and the aromatic proton signal of 1,3,5-trimethoxybenzene using increasing concentrations of formate. The amount of formate generated in the catalytic test was then determined using this calibration curve.

For the recyclability experiments, the photocatalyst was centrifuged and washed by water and ethanol after each circle illumination (4 h), respectively. Then the Schlenk tube was refilled 3 mL mixed solution of acetonitrile containing 1.5 M H_2O, 0.025 M BIH and 0.4 mM pySH, and the system was degassed with CO_2. Finally, the solution was irradiated under a 300

W Xenon lamp with an optical filter (λ ≥ 400 nm) for the next circle illumination.

7. DFT calculation details

Geometry optimization and frequency analysis were performed in acetonitrile solvent with the SMD implicit-solvation model using B3LYP-D3/def2-SVP level. Single point energies were calculated at the B3LYP-D3/def2-TZVP level with the SMD model (acetonitrile solvent) on optimized geometries.[5] The activation barriers are calculated using H_2O molecule as an explicit proton source. Time-dependent density functional theory (TDDFT) at the B3LYP-D3/def2-TZVP level of theory is used to model the electronic transitions on the COF fragment with Gaussian16. Hole-electron analysis was done to investigate the electronic excitation features with the aid of Multiwfn program.[6] The theoretical calculation of BDE values for S-H bond of thiol ligands were obtained by using DFT method M062X-D3/ def2-TZVP level. All of the theoretical calculations were performed with the Gaussian 16 program.[7]

8. $^{13}CO_2$ labeling experiment

The CH_3CN solution containing 1 mg Fe-bpy-COF, 0.4 mM pySH, 1.5 M H_2O and 0.025 M BIH was degassed by freeze-pump-thaw cycles and then $^{13}CO_2$ gas was introduced. The $^{13}CO_2$ gas is generated from purchased $Ba^{13}CO_3$ (abundance 98%). After irradiation for 4 h at 20 ºC with a 300 W Xe lamp equipped with an optical filter (λ ≥ 400 nm), the evolved CO was detected by a GCMS-QP2010 SE and the generated formate in the reaction solutions was quantified using ^{1}H NMR spectra on a Bruker AV400 spectrometer.

9. Quantum yield measurement

The rate of photon flux of the light was determined by a potassium ferrioxalate ($K_3[Fe(C_2O_4)_3]$) actinometer.[8] The incident light intensity was determined to be 1.519×10^{-7} einstein s^{-1} (for 420 nm) and 1.137×10^{-7} einstein s^{-1} (for 400 nm).[1]

3.0 mL of CH_3CN solution containing 1 mg Fe-bpy-COF, 0.4 mM pySH, 1.5 M H_2O and 0.025 M BIH was degassed by freeze-pump-thaw cycles and CO_2 was introduced. After irradiation for 1 h at 20 ºC with a 300 W Xe lamp equipped with a 400 nm band pass filter, the amount of the generated CO during catalysis was determined by GC and the amount of $HCOO^-$ was determined by ^{1}H NMR on a Bruker AV400 spectrometer. Quantum yield of the reaction was calculated by following equation:

$$\Phi(\%) = \frac{moles_{CO\ or\ HCOO^-} \times 2}{incident\ photons} \times 100\%$$

It can be found the amount of the generated CO and $HCOO^-$ was 0.25 μmol and 1.05 μmol respectively after 1 h of irradiation under 420 nm light. And the generated CO and $HCOO^-$ was 1.07 μmol and 2.56 μmol respectively after 1 h of irradiation under 400 nm light. The quantum yield was estimated to be $\Phi_{CO} = 0.09\%$ and $\Phi_{HCOO^-} = 0.38\%$ under 420 nm light. The quantum yield was estimated to be $\Phi_{CO} = 0.52\%$ and $\Phi_{HCOO^-} = 1.25\%$ under 400 nm light.

10. Supplementary figures and tables

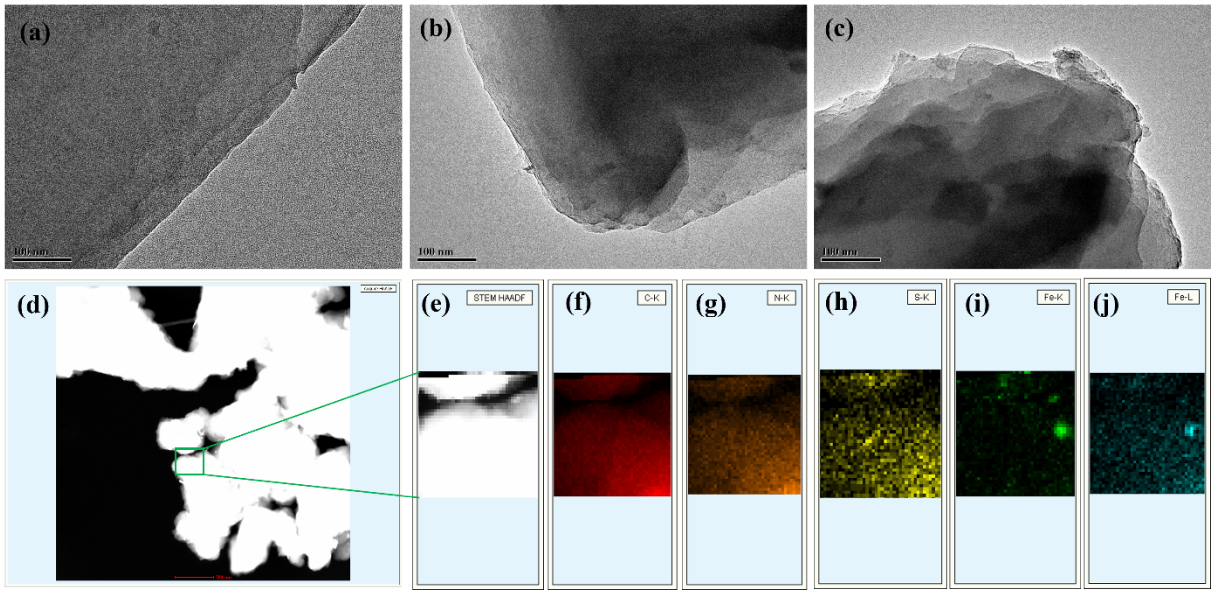

Figure S1. TEM image of (a) bpy-COF, (b) Fe-bpy-COF, (c) FeS-bpy-COF, and (d-j) element mapping of FeS-bpy-COF.

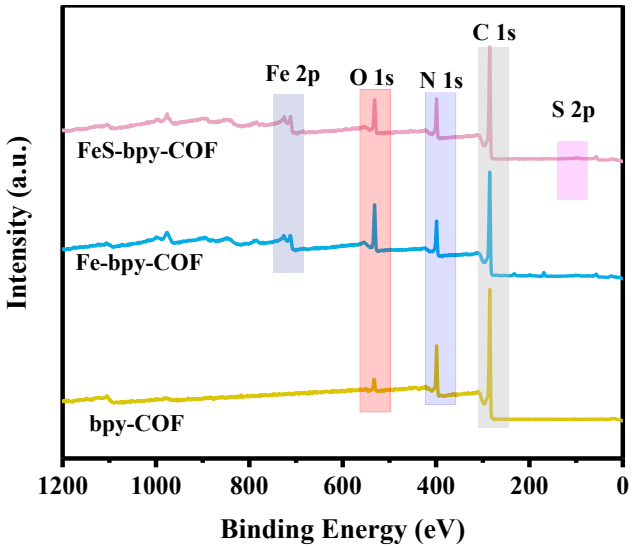

Figure S2. The total XPS profiles of bpy-COF, Fe-bpy-COF and FeS-bpy-COF.

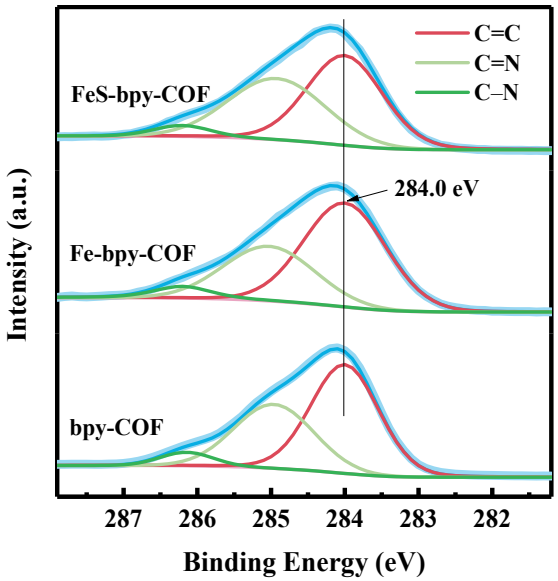

Figure S3. C 1s XPS spectra of bpy-COF, Fe-bpy-COF and FeS-bpy-COF.

Table S1. N_2 and CO_2 physisorption results of bpy-COF and FeS-bpy-COF.

Sample	S_{BET} (m^2 g^{-1})	V_{total} (cm^3 g^{-1})	V_{micro} (cm^3 g^{-1})	CO_2 (cm^3 g^{-1})		Q_{st}(kJ mol^{-1})
				0 °C	25 °C	
bpy- COF	173.7	0.191	0.062	10.6	5.3	28.4
FeS-bpy- COF	123.3	0.170	0.025	9.7	6.6	20.1

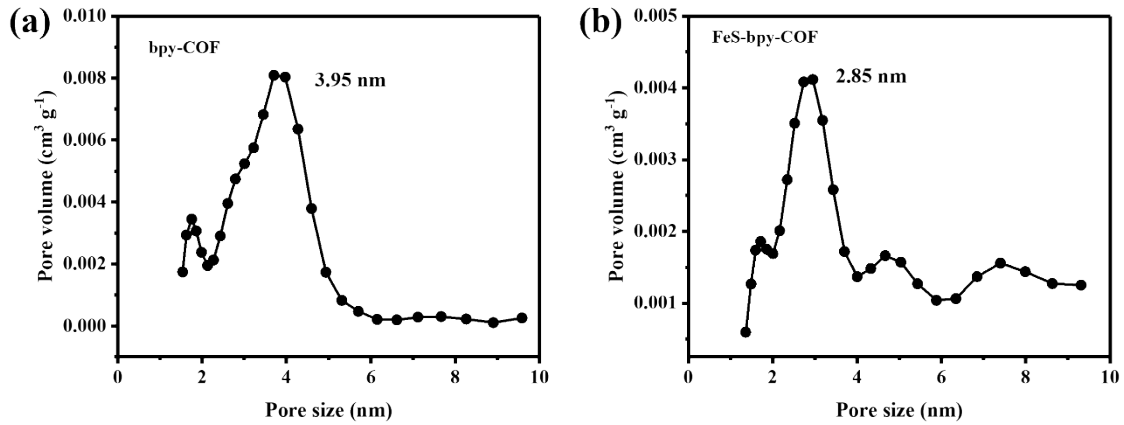

Figure S4. Pore size distribution profile (a) bpy-COF, (b) FeS-bpy-COF

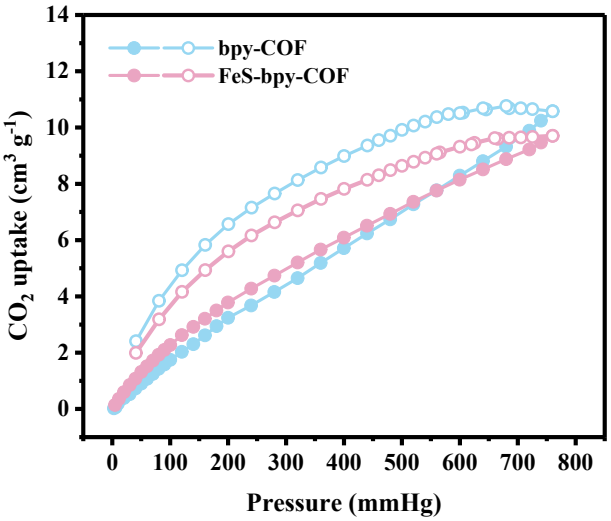

Figure S5. CO_2 adsorption isotherm patterns at 0 °C

Table S2. Elemental analysis experimental and predictive results

Sample	Mass percentage of different elements (%)		
	N	C	H
bpy-COF	18.38	70.44	4.70
Fe-bpy-COF	17.77	65.54	4.39
FeS-bpy-COF	17.53	66.56	4.03

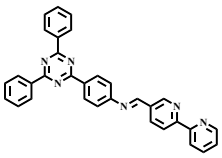

Elemental Analysis: C, 78.35; H, 4.52; N, 17.13

bpy-COF

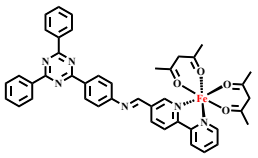

Elemental Analysis: C, 67.56; H, 5.13; Fe, 7.48; N, 11.26; O, 8.57

Fe-bpy-COF

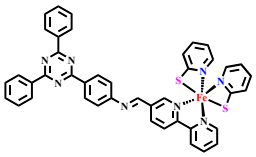

Elemental Analysis: C, 65.79; H, 3.94; Fe, 7.28; N, 14.61; S, 8.36

FeS-bpy-COF

Table S3. ICP-OES results of Fe-bpy-COF and FeS-bpy-COF.

Sample	Fe (wt%)	S (wt%)
Fe-bpy-COF	2.77	-
FeS-bpy-COF	2.41	0.375

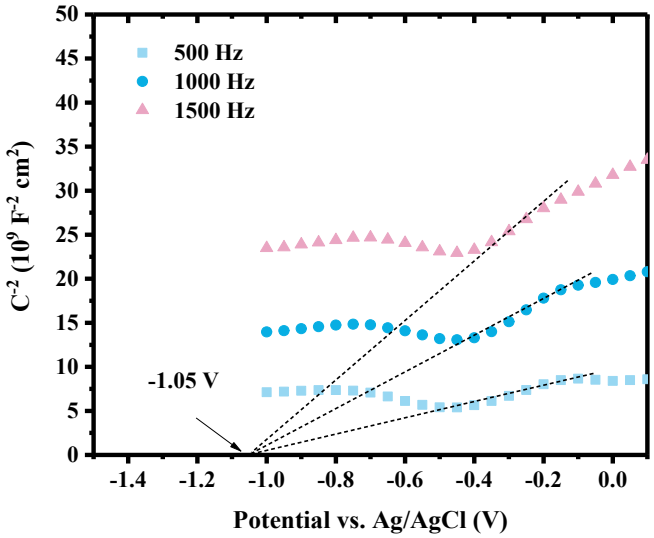

Figure S6. Mott−Schottky plots of bpy-COF.

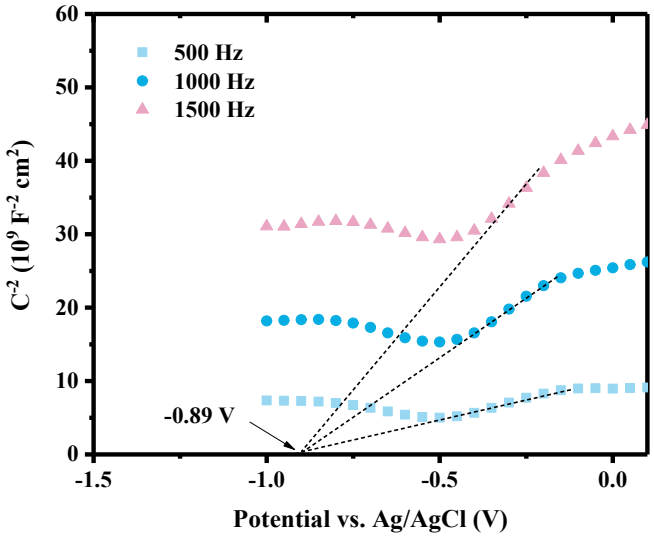

Figure S7. Mott−Schottky plots of Fe-bpy-COF.

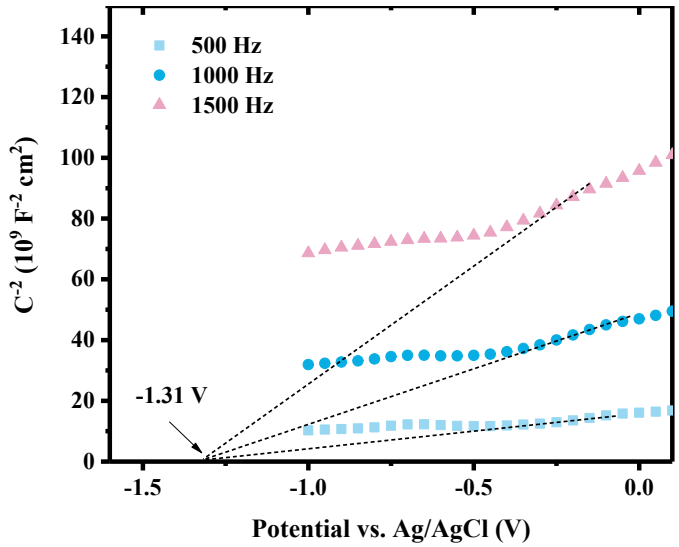

Figure S8. Mott−Schottky plots of FeS-bpy-COF.

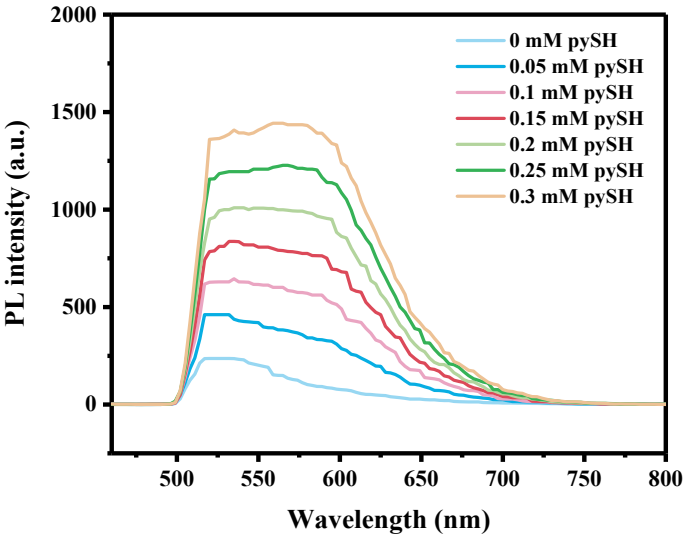

Figure S9. PL spectra of different pySH concentrations in CH_3CN (Ex: 440 nm, with 510nm filter).

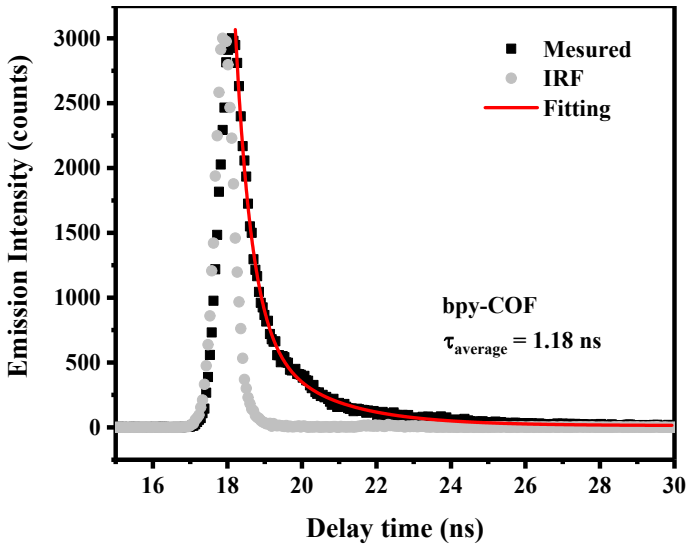

Figure S10. Time-resolved photoluminescence decay spectra of bpy-COF with 450 nm laser.

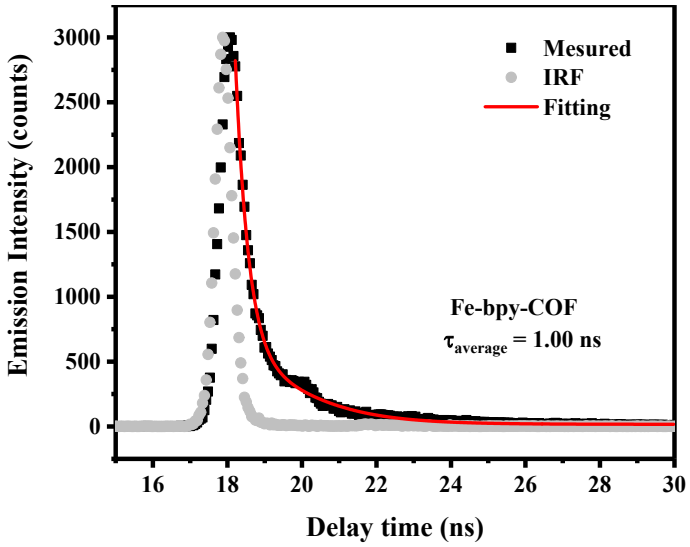

Figure S11. Time-resolved photoluminescence decay spectra of Fe-bpy-COF with 450 nm laser.

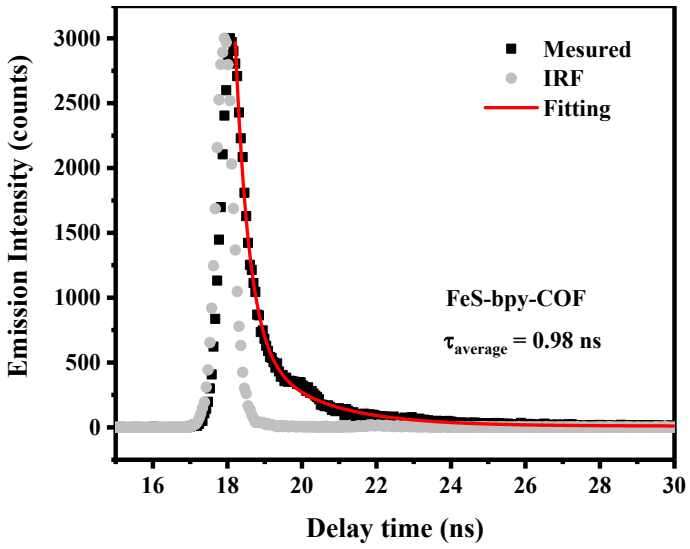

Figure S12. Time-resolved photoluminescence decay spectra of FeS-bpy-COF with 450 nm laser.

Table S4. Fluorescence lifetime test results

Sample	Lifetime(ns)	Coefficient	Lifetime average(ns)
bpy-COF	$\tau_1 = 0.44$	$A_1 = 0.145$	$\tau_{average} = 1.18$
	$\tau_2 = 2.53$	$A_2 = 0.014$	
Fe-bpy-COF	$\tau_1 = 0.31$	$A_1 = 0.190$	$\tau_{average} = 1.00$
	$\tau_2 = 2.15$	$A_2 = 0.017$	
FeS-bpy-COF	$\tau_1 = 0.31$	$A_1 = 0.184$	$\tau_{average} = 0.98$
	$\tau_2 = 2.08$	$A_2 = 0.017$	

Table S5. The fitting parameters for the kinetic traces at 610 nm in fs-TA

Sample	τ_1, ps (A_1,%)	τ_2, ps (A_2,%)	τ_3, ps (A_3,%)	τ_{avg}, ps
bpy-COF	1.32(65.7)	24.3 (18.3)	1990 (16.0）	323.71
Fe-bpy-COF	1.09 (63.3)	19.2 (24.6)	2440 (12.1)	300.65
FeS-bpy-COF	1.10 (46.8)	23.7 (37.3)	2550 (15.9)	414.80

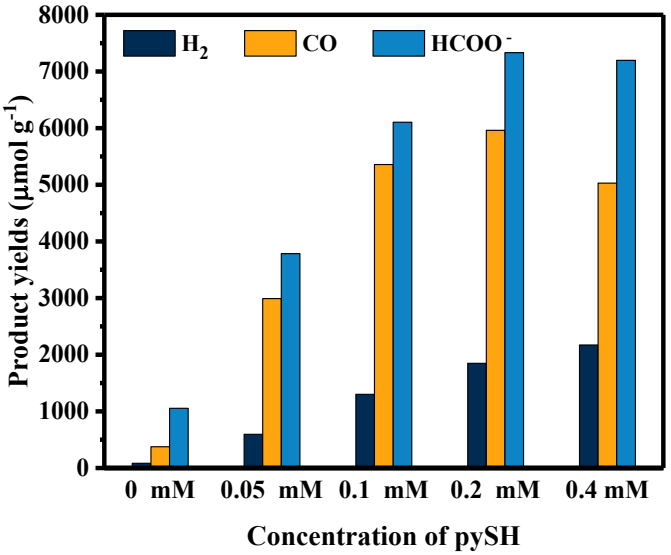

Figure S13. The product yields catalyzed by FeS-bpy-COF with additional different concentrations of pySH.

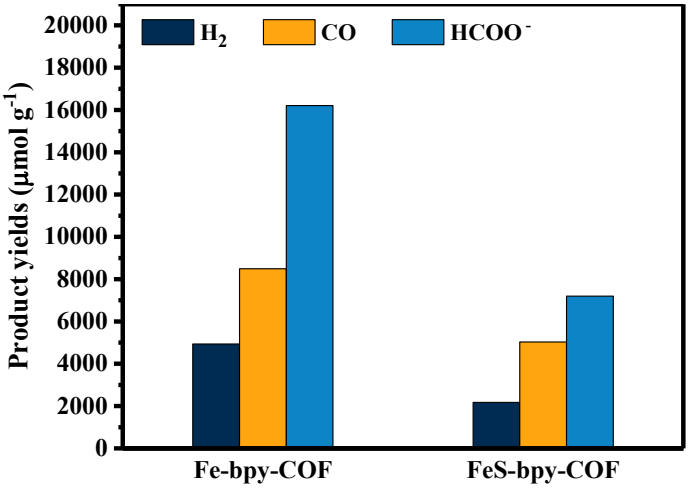

Figure S14. The product yields catalyzed by Fe-bpy-COF or FeS-bpy-COF with additional 0.4 mM pySH.

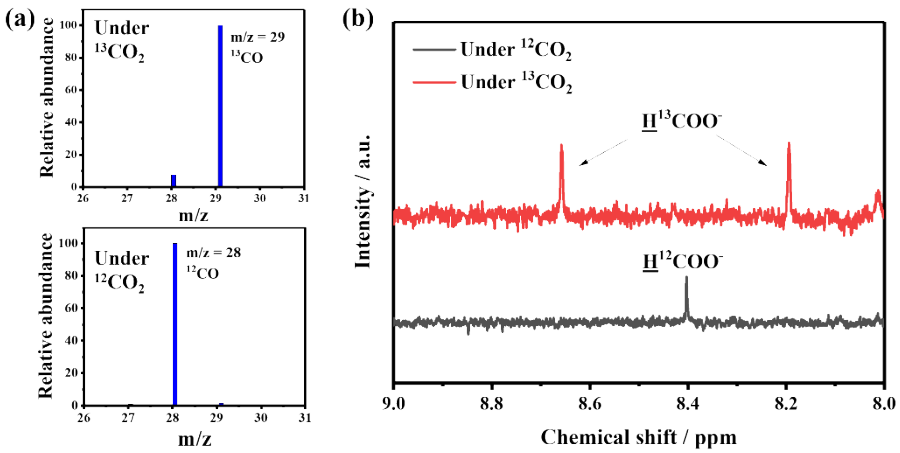

Figure S15. Isotopic labeling experiment (a) Mass spectra of CO, and (b) ^{1}H NMR spectra of $HCOO^-$ generated under $^{12}CO_2$ or $^{13}CO_2$.

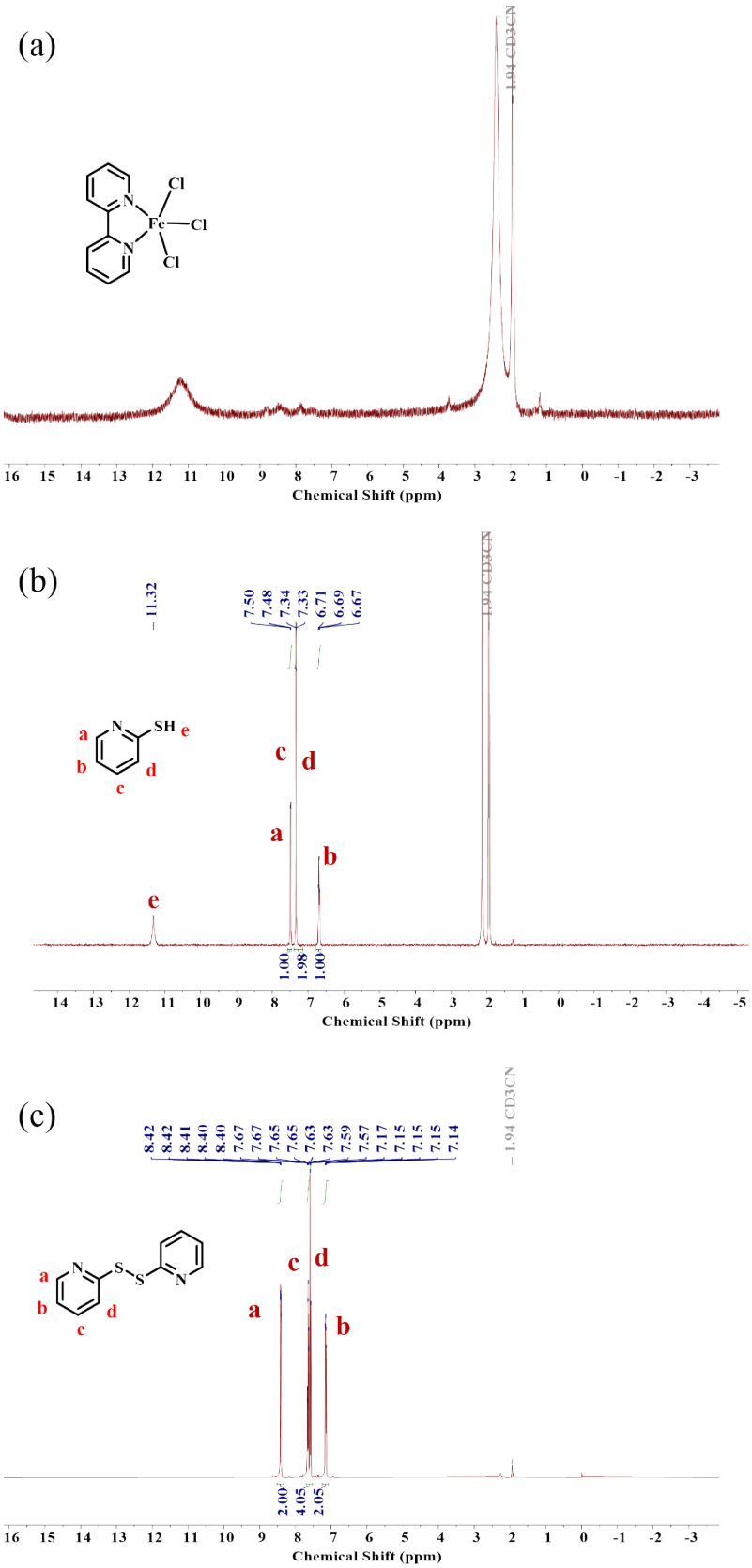

Figure S16. ^{1}H NMR spectra in CD_3CN, (a) $FebpyCl_3$, (b) pySH, (c) pyS-Spy.

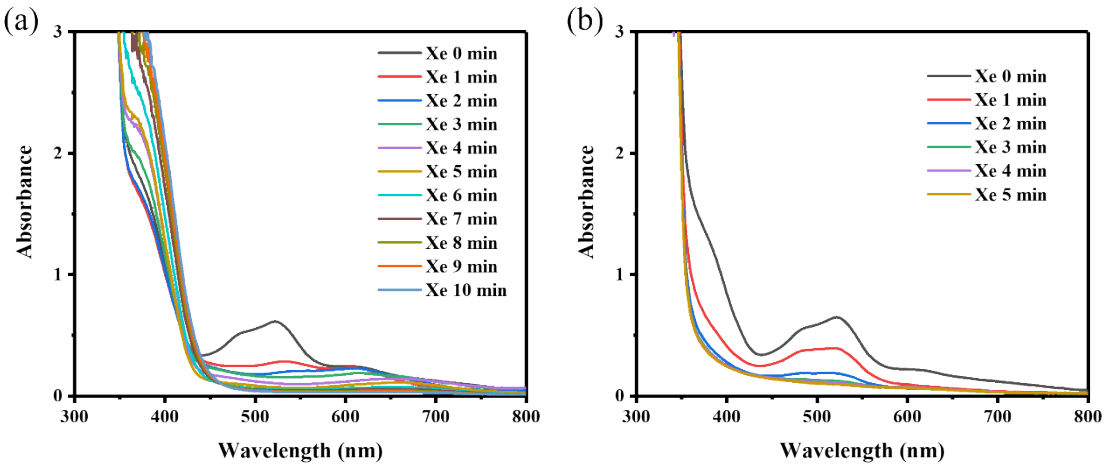

Figure S17. Steady-state measurements of absorption spectral in CH_3CN solution containing 0.2 mM $FebpyCl_3$, 0.4 mM pySH, 0.025 M BIH and 1.5 M H_2O upon photo-irradiation under (a) CO_2 and (b) Ar.

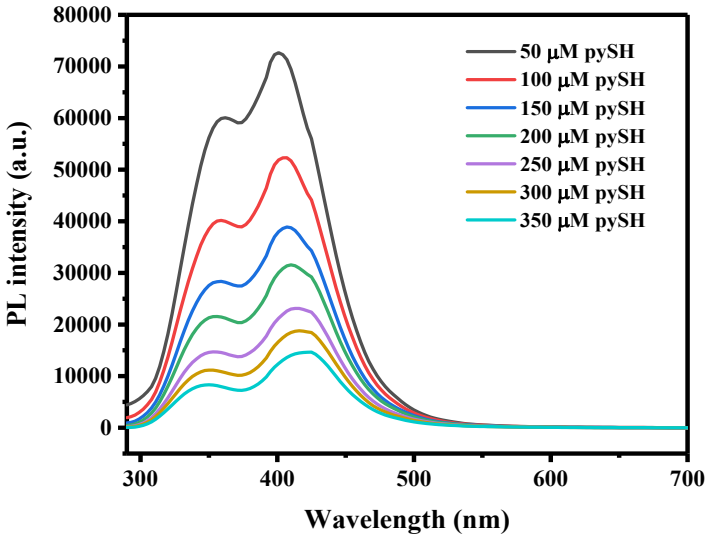

Figure S18. PL spectra of different pySH concentrations in CH_3CN (Ex: 270 nm).

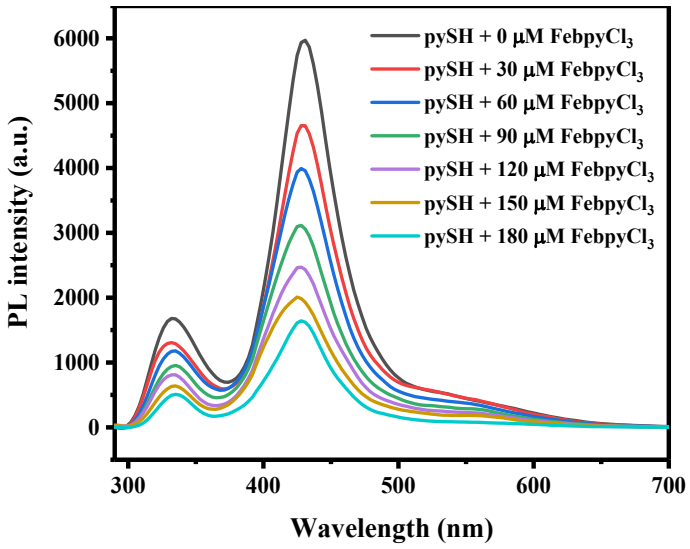

Figure S19. PL spectra of 0.6 mM pySH with different $FebpyCl_3$ concentrations in CH_3CN (Ex: 270 nm).

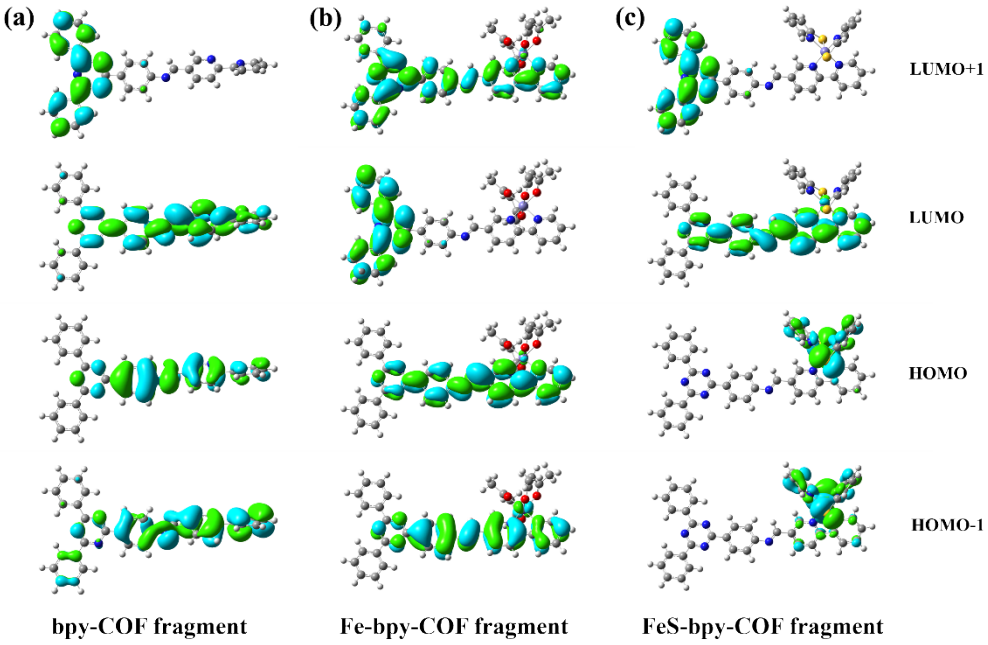

Figure S20. Frontier molecular orbitals of (a) bpy-COF fragment; (b) Fe-bpy-COF fragment; (c) FeS-bpy-COF fragment.

Table S6. Transferred electrons between fragments

Donor fragment	Acceptor fragment			
	1	**2**	**3**	**4**
1	0.004	**0.012**	0.216	0.080
2	0.009	0.026	**0.456**	0.170
3	0.000	0.000	0.018	0.007
4	0.000	0.000	0.000	0.000

Table S7. Variation of different fragments population number

Fragment	**1**	**2**	**3**	**4**
Variation of population number	-0.298	-0.621	0.664	0.256

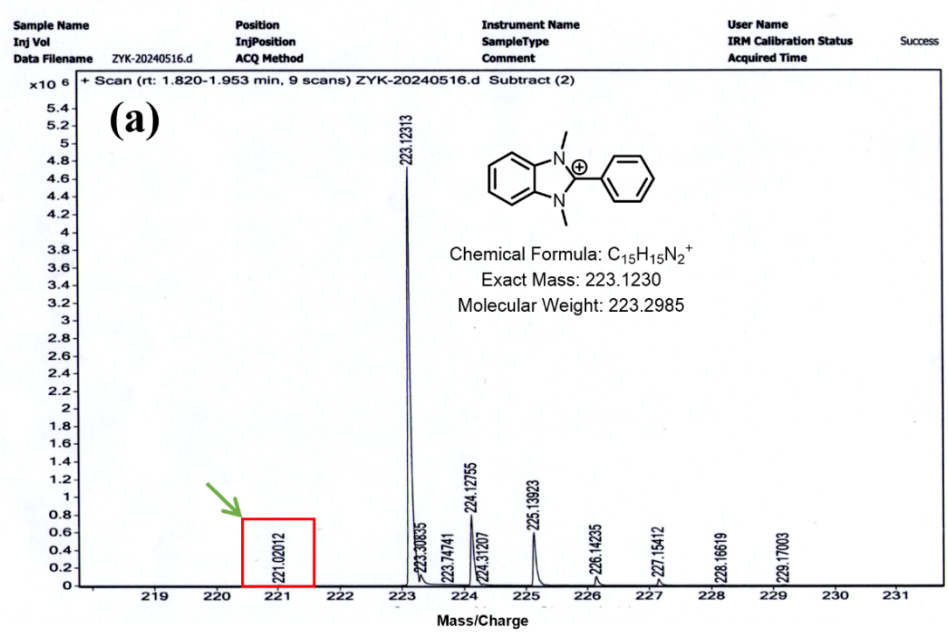

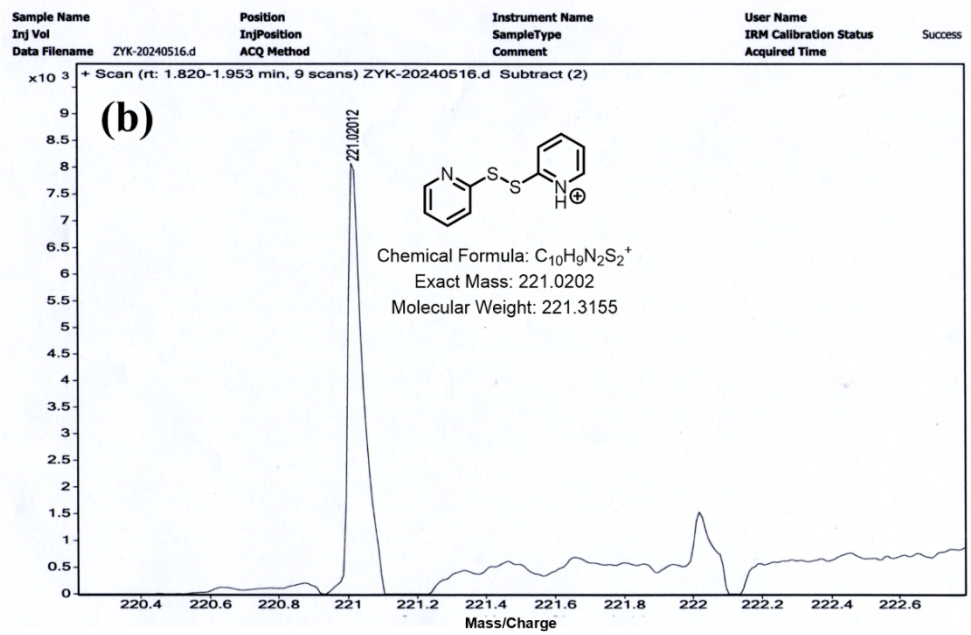
Sample Name
Inj Vol
Data Filename ZYK-20240516.d
Position
InjPosition
ACQ Method
Instrument Name
SampleType
Comment
User Name
IRM Calibration Status Success
Acquired Time
+ Scan (rt: 1.820-1.953 min, 9 scans) ZYK-20240516.d Subtract (2)
x10 3
(b)
221.02012
Chemical Formula: $C_{10}H_9N_2S_2^+$
Exact Mass: 221.0202
Molecular Weight: 221.3155
Mass/Charge

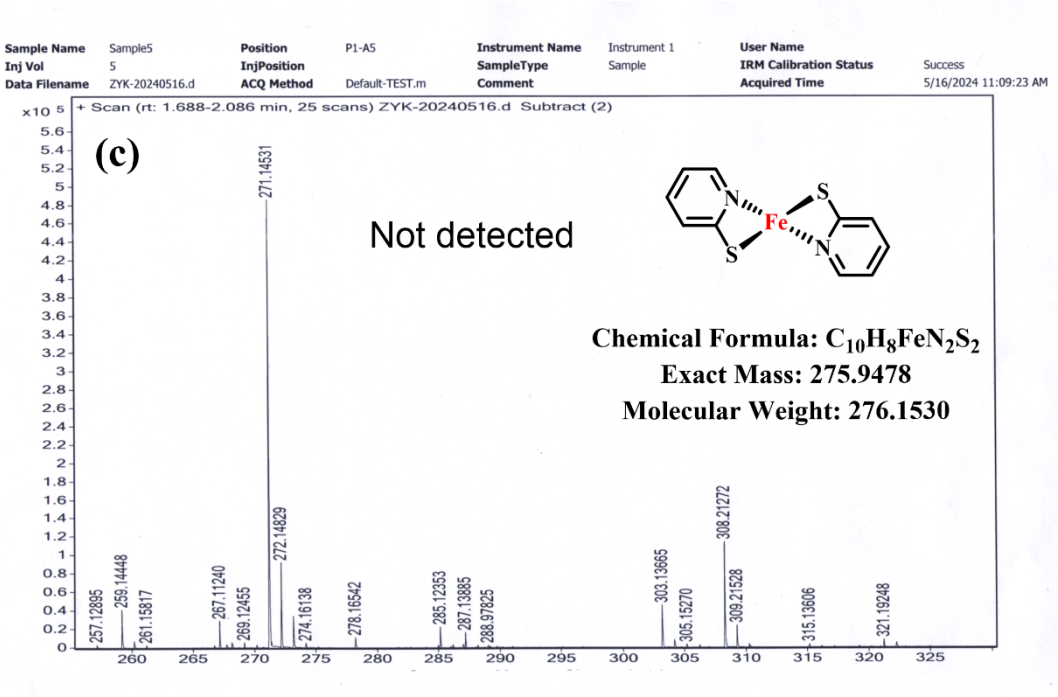
Sample Name Sample5
Inj Vol 5
Data Filename ZYK-20240516.d
Position P1-A5
InjPosition
ACQ Method Default-TEST.m
Instrument Name Instrument 1
SampleType Sample
Comment
User Name
IRM Calibration Status Success
Acquired Time 5/16/2024 11:09:23 AM
+ Scan (rt: 1.688-2.086 min, 25 scans) ZYK-20240516.d Subtract (2)
x10 5
(c)
271.14531
272.14829
Not detected
Chemical Formula: $C_{10}H_8FeN_2S_2$
Exact Mass: 275.9478
Molecular Weight: 276.1530
257.12895
259.14448
261.15817
267.11240
269.12455
274.16138
278.16542
285.12353
287.13885
288.97825
303.13665
305.15270
308.21272
309.21528
315.13606
321.19248

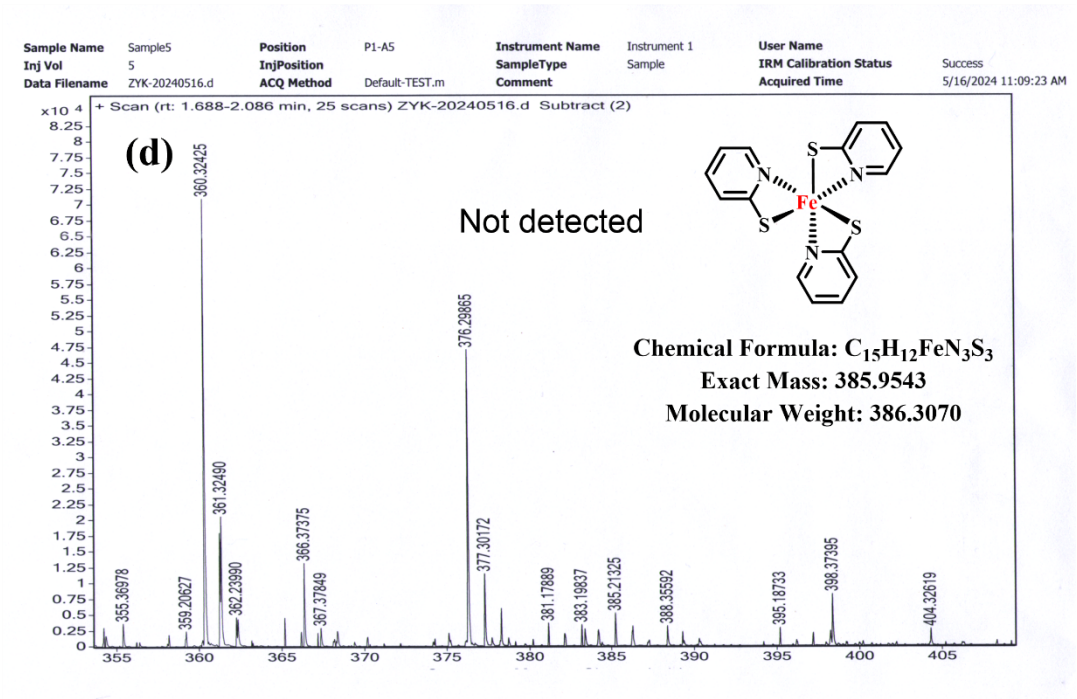

Figure S21. High-resolution mass spectrometry results of the solution after 1h reaction for Fe-bpy-COF with 2 mM pySH system. (a) Mass spectra of m/z from 218 to 232; (b) View of the mass spectrometry with localized zoom in the red box; (c) Mass spectra of m/z from 255 to 330; (d) Mass spectra of m/z from 353 to 410.

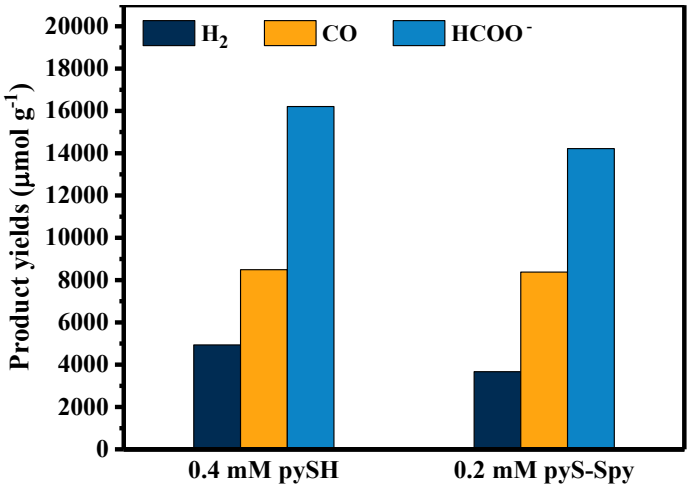

Figure S22. The product yields catalyzed by Fe-bpy-COF with additional 0.4 mM pySH or 0.2 mM pyS-Spy.

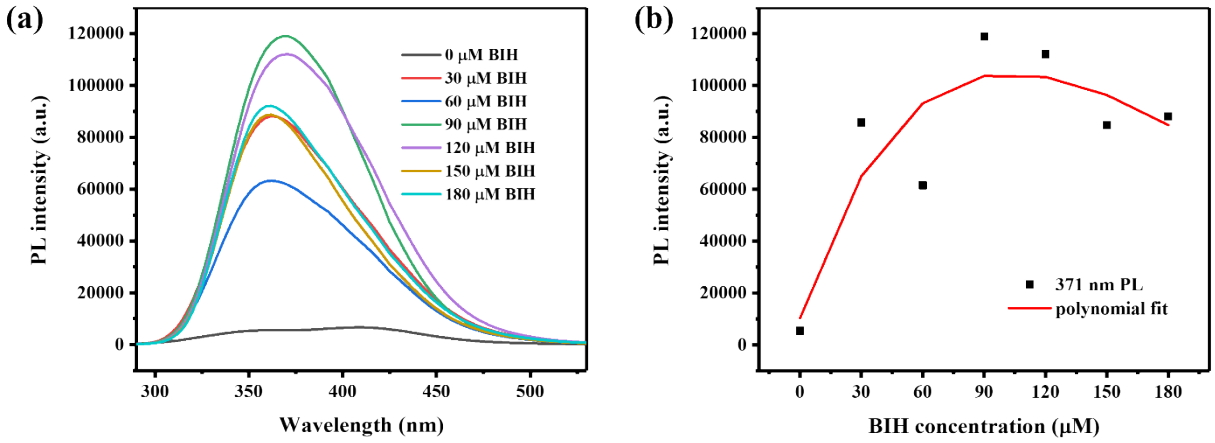

Figure S23. (a) PL spectra of 0.3 mM pyS-Spy with different BIH concentrations in CH_3CN (Ex: 270 nm). (b) The relationship between PL intensity at 371 nm and BIH concentration fitted by polynomial method

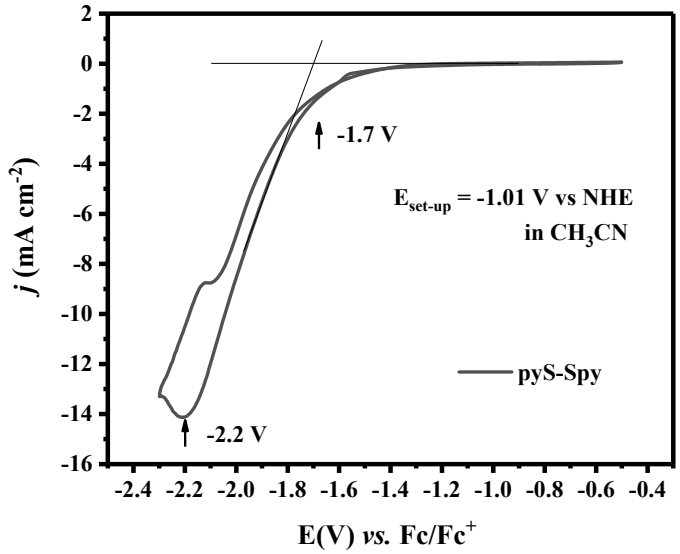

Figure S24. Cyclic voltammograms of 20 mM pyS-Spy in CH_3CN solution containing 0.1 M $TBAPF_6$ at scan rate 0.1 V/s under argon.

Table S8. BDE values obtained by theoretical calculations for BIH and thiol ligands.

Entry	abbreviation	Δ*H* kcal/mol	Entry	abbreviation	Δ*H* kcal/mol
1	pySH	88.4	8	CF_3-pySH	90.2
2	CH_3-pySH	84.9	9	CH_3-phSH	78.6
3	NH_2-pySH	91.0	10	NO-pySH	87.0
4	COOH-pySH	83.8	11	NO-pyOH	69.9
5	Cl-pySH	85.8	12	4-pySH	86.8
6	CN-pySH	88.2	13	2-phOHSH	80.5
7	NO_2-pySH	88.4	/	BIH	71.5

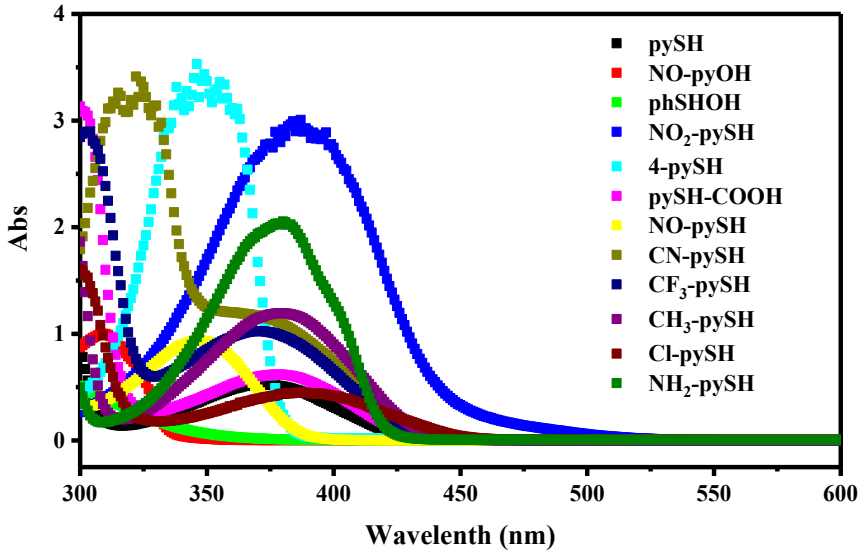

Figure S25. UV-vis spectra of 0.2 mM pySH with different substituents in CH_3CN.

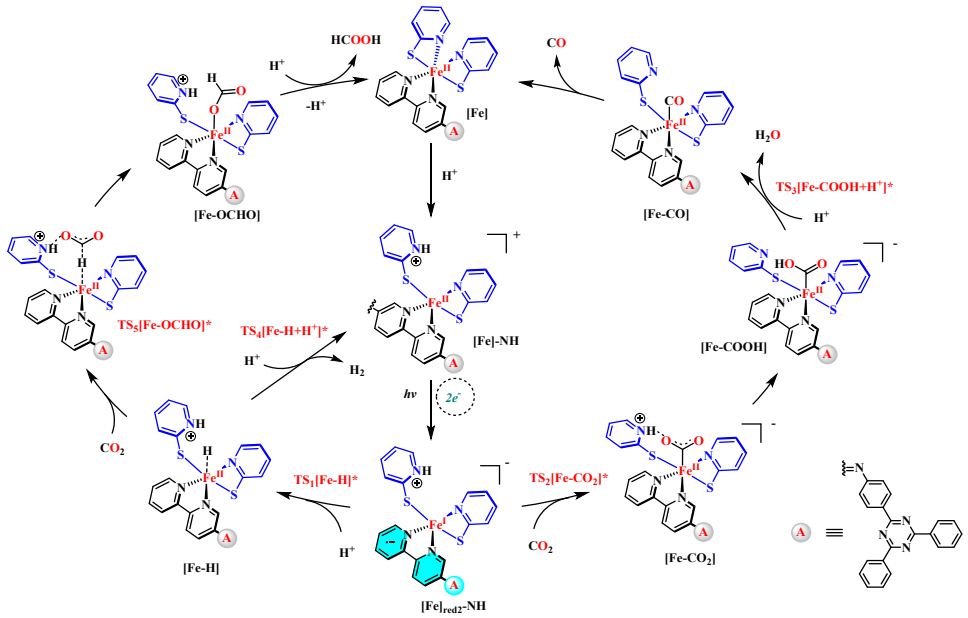

Scheme S1. Proposed catalytic mechanism for photocatalytic CO_2 reduction by FeS-bpy-COF.

11. The coordinates of transition states in DFT calculation (in xyz format)

TS_1[Fe-H]*

-1 3

C	-5.456113	-2.792417	-0.859482
C	-7.609650	-1.903879	-0.575150
C	-8.213991	-3.045704	-1.089872
C	-7.385164	-4.106039	-1.500332
C	-6.008813	-3.983981	-1.386772
C	-4.045750	-2.531610	-0.699057
C	-2.475751	-0.927701	-0.008691
C	-1.371420	-1.749943	-0.342590
C	-1.682179	-3.041547	-0.881631
C	-2.995115	-3.415415	-1.054454
H	-8.205036	-1.052855	-0.236949
H	-7.820276	-5.022165	-1.907472
H	-5.355121	-4.798090	-1.700779
H	-2.310826	0.069888	0.405795
H	-0.865041	-3.712171	-1.152488
H	-3.233327	-4.394987	-1.471701
N	-3.737663	-1.294350	-0.167993
N	-6.281465	-1.778168	-0.461151
Fe	-5.289253	-0.188908	0.336573
C	-6.874234	0.139318	2.376374
C	-7.865053	0.486727	3.312848
C	-8.832941	1.414889	2.939742
C	-8.808616	1.977849	1.652281
C	-7.799008	1.590123	0.777804
N	-6.861077	0.703704	1.143107
H	-9.614872	1.700951	3.648208
H	-7.863298	0.026365	4.302641
H	-9.561182	2.700077	1.331958
H	-7.733184	1.978462	-0.241149
C	-5.081517	4.424427	0.020297
C	-5.287832	5.342347	-0.985255
C	-5.485107	4.857977	-2.296478
C	-5.479348	3.497606	-2.555453
C	-5.276067	2.575038	-1.500573
N	-5.079688	3.102075	-0.262928
H	-5.647506	5.561645	-3.116682
H	-4.914209	4.690064	1.065353
H	-5.294217	6.409258	-0.761247
H	-5.637146	3.114872	-3.564615

S	-5.563085	-1.001206	2.536099
S	-5.265949	0.862981	-1.748062
C	2.294813	-1.516531	-0.302211
C	3.361284	-2.457384	-0.246373
C	2.651584	-0.135488	-0.282722
C	4.682740	-2.056335	-0.145429
H	3.104165	-3.519465	-0.275537
C	3.976661	0.260543	-0.191493
H	1.876330	0.628744	-0.366877
C	5.027495	-0.683532	-0.113131
H	5.475570	-2.804104	-0.093334
H	4.221276	1.324021	-0.187745
C	6.426817	-0.253871	-0.015859
C	8.646931	-0.763252	0.149393
C	7.984686	1.413623	0.074861
C	8.321304	2.864037	0.080894
C	9.660315	3.286613	0.175485
C	7.305266	3.833922	-0.007951
C	9.974589	4.646905	0.181378
H	10.451145	2.538819	0.244601
C	7.622054	5.193316	-0.002050
H	6.266163	3.510926	-0.082032
C	8.957210	5.604423	0.092612
H	11.018667	4.962009	0.255600
H	6.823554	5.936607	-0.071911
C	9.733770	-1.776837	0.241518
C	9.431138	-3.151305	0.247534
C	11.079969	-1.375053	0.324366
C	10.451196	-4.100195	0.334279
H	8.389232	-3.467373	0.184391
C	12.098437	-2.326064	0.410752
H	11.319222	-0.311022	0.320304
C	11.787791	-3.691079	0.415956
H	10.202916	-5.164731	0.338275
H	13.140130	-2.000927	0.474401
C	-0.040246	-1.274434	-0.140476
H	0.045456	-0.254770	0.274528
H	12.586051	-4.435093	0.483867
H	9.204157	6.669464	0.097233
N	6.699210	1.065707	-0.010856
N	8.993482	0.532806	0.156566
N	7.387081	-1.195630	0.064379
N	1.017362	-2.009181	-0.402059
H	-9.300879	-3.104387	-1.165746

H	-4.893350	2.407709	0.485257
H	-4.462947	0.946190	0.961570

Thermal correction to Gibbs Free Energy= 0.5675870 (A.U.)
Electronic Energy= -4194.9069420 (A.U.)
The number of imaginary frequencies: 1

TS_2[Fe-CO_2]*

-1 1

C	-7.413643	-0.625363	-2.073837
N	-6.140078	-0.711437	-1.647239
C	-5.361196	-1.758220	-2.076195
C	-5.916605	-2.783704	-2.878500
C	-7.238393	-2.702543	-3.279924
C	-8.004166	-1.589042	-2.881425
Fe	-5.206274	0.596867	-0.507795
N	-3.620498	-0.476427	-1.115052
C	-2.341274	-0.244591	-0.841258
C	-1.294559	-1.141403	-1.132455
C	-1.663762	-2.410508	-1.678936
C	-2.989176	-2.666823	-1.938777
C	-3.974790	-1.673449	-1.703028
S	-4.997998	-0.937134	1.341707
C	-6.156510	-1.115026	2.571138
N	-7.282263	-0.338842	2.707927
C	-8.216558	-0.497337	3.674073
C	-8.098578	-1.483232	4.621332
C	-6.949535	-2.318801	4.555410
C	-6.010757	-2.138464	3.567293
S	-5.192449	2.379526	-2.045293
C	-4.159540	2.964212	-0.781552
N	-4.080422	2.047873	0.215653
C	-3.398725	2.299799	1.334431
C	-2.692015	3.488382	1.507673
C	-2.730614	4.441233	0.475296
C	-3.470413	4.189458	-0.676347
H	-5.125820	-2.772644	3.500402
H	-6.810442	-3.111549	5.295680
H	-8.859931	-1.607175	5.391460
H	-9.047192	0.210292	3.635592
H	-3.537240	4.913645	-1.490264
H	-2.187235	5.385235	0.579721
H	-2.134661	3.668412	2.428749
H	-3.433444	1.516952	2.096571

H	-2.120722	0.706927	-0.352308
H	-0.880583	-3.146817	-1.865055
H	-3.290669	-3.637247	-2.338221
H	-5.289418	-3.616311	-3.199966
H	-7.673843	-3.485531	-3.907052
H	-9.050243	-1.481177	-3.175033
H	-7.957666	0.234741	-1.679927
C	-6.758901	1.555659	0.565792
O	-6.467299	2.177484	1.590941
O	-7.863605	1.199162	0.120370
H	-7.394924	0.456698	2.067215
C	0.060737	-0.776864	-0.834596
H	0.199075	0.235628	-0.408759
N	1.062650	-1.592543	-1.010590
C	2.366969	-1.221526	-0.803148
C	2.853815	0.118627	-0.798304
C	3.324449	-2.256060	-0.614054
C	4.194379	0.392984	-0.589001
H	2.165065	0.943691	-0.991408
C	4.661336	-1.978645	-0.395263
H	2.958585	-3.285159	-0.636443
C	5.134699	-0.643220	-0.373184
H	4.550570	1.424281	-0.596847
H	5.375717	-2.788099	-0.239200
C	6.544644	-0.345592	-0.149824
C	8.242546	1.168618	0.064050
C	8.681431	-1.051423	0.245407
C	8.713110	2.582535	0.075268
C	7.805587	3.637032	-0.127067
C	10.069951	2.881672	0.288317
C	8.246600	4.960855	-0.116437
H	6.754944	3.394886	-0.291233
C	10.508788	4.206870	0.298444
H	10.766470	2.057265	0.444549
C	9.599449	5.250888	0.096236
H	7.531074	5.772185	-0.274844
H	11.566777	4.427358	0.465179
H	9.943802	6.288814	0.104379
C	9.651306	-2.162210	0.463355
C	11.013055	-1.888978	0.679220
C	9.216510	-3.499047	0.455952
C	11.919723	-2.930769	0.883159
H	11.340819	-0.848898	0.683231
C	10.124613	-4.538721	0.660066

H	8.157877	-3.700253	0.287727
C	11.479323	-4.258811	0.874390
H	12.976754	-2.705900	1.050098
H	9.774280	-5.574412	0.652177
H	12.190081	-5.074435	1.034289
N	6.948137	0.945508	-0.143619
N	9.157814	0.204763	0.265132
N	7.406058	-1.370619	0.044924

Thermal correction to Gibbs Free Energy= 0.5644310 (A.U.)
Electronic Energy= -4307.1042456 (A.U.)
The number of imaginary frequencies: 1

TS_3[Fe-COOH+H^+]*

-1 1

C	-5.150906	-2.364067	-0.095679
C	-7.098254	-1.581333	0.904307
C	-7.807731	-2.714669	0.526838
C	-7.155274	-3.702022	-0.222488
C	-5.809196	-3.530616	-0.518024
C	-3.719379	-2.133686	-0.219256
C	-1.995700	-0.727437	0.454443
C	-1.010938	-1.571792	-0.081963
C	-1.439823	-2.755874	-0.730694
C	-2.792345	-3.033086	-0.786769
H	-7.579044	-0.777175	1.454288
H	-7.688791	-4.593005	-0.563432
H	-5.261521	-4.293913	-1.072207
H	-1.718007	0.204197	0.952856
H	-0.693444	-3.423751	-1.164035
H	-3.147166	-3.944865	-1.268785
N	-3.300211	-0.978393	0.376191
N	-5.816674	-1.371411	0.564833
Fe	-4.809301	0.277265	0.764519
C	-3.475419	1.631604	2.578528
C	-2.678957	2.539131	3.315226
C	-2.040941	3.573782	2.641720
C	-2.200124	3.711911	1.250903
C	-2.998086	2.782178	0.586325
N	-3.584975	1.772471	1.230797
H	-1.423418	4.287146	3.196933
H	-2.592142	2.414056	4.396274
H	-1.726552	4.526824	0.699851

H	-3.194775	2.824820	-0.489273
C	-8.351014	-0.545419	-2.521035
C	-9.031033	0.560396	-3.038277
C	-8.329450	1.769347	-3.121234
C	-7.013225	1.817864	-2.675620
C	-6.412116	0.648966	-2.151008
N	-7.087196	-0.513566	-2.100295
H	-8.812182	2.669684	-3.515764
H	-8.868640	-1.507161	-2.420767
H	-10.073930	0.474611	-3.352968
H	-6.437526	2.744876	-2.691300
S	-4.393421	0.285830	3.153067
S	-4.750020	0.705442	-1.558597
C	2.664764	-1.495445	-0.375369
C	3.679260	-2.457614	-0.158820
C	3.058291	-0.151639	-0.590477
C	5.015771	-2.090795	-0.115965
H	3.375154	-3.496555	-0.015552
C	4.398860	0.209871	-0.558532
H	2.297798	0.600414	-0.811455
C	5.403598	-0.748102	-0.313968
H	5.788683	-2.838333	0.066199
H	4.692802	1.246194	-0.729621
C	6.822067	-0.359474	-0.277915
C	9.018619	-0.914515	-0.018617
C	8.438043	1.242520	-0.433087
C	8.824750	2.663236	-0.648172
C	10.176768	3.047036	-0.616459
C	7.841241	3.639481	-0.885275
C	10.536569	4.380149	-0.818041
H	10.933195	2.283624	-0.431652
C	8.203967	4.971735	-1.086349
H	6.794827	3.333474	-0.907648
C	9.551954	5.346284	-1.053470
H	11.590804	4.668298	-0.791311
H	7.431061	5.722638	-1.269375
C	10.065121	-1.941925	0.236212
C	9.707510	-3.286633	0.436663
C	11.423001	-1.581013	0.279984
C	10.688839	-4.249394	0.675661
H	8.651768	-3.557469	0.401341
C	12.402288	-2.545960	0.519424
H	11.691497	-0.535723	0.123756
C	12.038714	-3.882603	0.717883

H	10.399671	-5.292169	0.830316
H	13.455482	-2.254608	0.551777
C	0.385587	-1.199064	0.035929
H	0.581078	-0.245007	0.564486
H	12.806690	-4.637968	0.905568
H	9.834722	6.390682	-1.210980
N	7.140781	0.932296	-0.477051
N	9.415229	0.352181	-0.206854
N	7.744565	-1.311185	-0.045476
N	1.349766	-1.925706	-0.415336
H	-8.867838	-2.770024	0.775130
C	-6.293749	1.585522	0.968718
O	-7.598962	1.257210	0.497780
O	-6.214604	2.725014	1.386754
H	-8.079195	2.100493	0.602597
O	-9.891109	-0.446455	0.203862
H	-9.013786	-0.029150	0.096304
H	-10.453513	0.311599	0.407389

Thermal correction to Gibbs Free Energy= 0.5887030 (A.U.)
Electronic Energy= -4383.6259088 (A.U.)
The number of imaginary frequencies: 1

TS_4[Fe-H+H^+]*

0 1

C	-5.554520	-2.836540	-0.966521
C	-7.673420	-1.973567	-0.525263
C	-8.292024	-3.079751	-1.100414
C	-7.497325	-4.106784	-1.622392
C	-6.111776	-3.980648	-1.555046
C	-4.113646	-2.574773	-0.853666
C	-2.531889	-1.049771	-0.093392
C	-1.468206	-1.841251	-0.543588
C	-1.774494	-3.061191	-1.178603
C	-3.103423	-3.426368	-1.331863
H	-8.248710	-1.149934	-0.101128
H	-7.950507	-4.990384	-2.077021
H	-5.466486	-4.762523	-1.956264
H	-2.343476	-0.095754	0.402652
H	-0.967540	-3.700880	-1.540113
H	-3.361695	-4.364895	-1.822671
N	-3.814437	-1.399668	-0.240536
N	-6.335997	-1.850012	-0.446723

Fe	-5.391997	-0.369465	0.397699
C	-4.319515	0.228737	2.726980
C	-3.667875	0.806528	3.838297
C	-3.078892	2.059595	3.700421
C	-3.137818	2.725508	2.463621
C	-3.794142	2.097967	1.408045
N	-4.369434	0.893521	1.539146
H	-2.570891	2.522070	4.551433
H	-3.636022	0.262253	4.784557
H	-2.682626	3.707353	2.321186
H	-3.859992	2.555865	0.417679
C	-7.406328	3.696397	-0.026890
C	-7.358356	4.762372	-0.897480
C	-6.599384	4.618088	-2.083859
C	-5.925102	3.441315	-2.354289
C	-5.979353	2.362287	-1.431265
N	-6.724000	2.565565	-0.309223
H	-6.547635	5.445195	-2.796927
H	-7.983711	3.671100	0.898544
H	-7.899804	5.681766	-0.672872
H	-5.340849	3.320440	-3.267692
S	-5.128169	-1.304169	2.637126
S	-5.173881	0.859650	-1.622651
C	2.219625	-1.556219	-0.620094
C	3.249402	-2.485160	-0.363750
C	2.559455	-0.195028	-0.780546
C	4.567587	-2.064609	-0.232093
H	2.988332	-3.540871	-0.260941
C	3.882268	0.218864	-0.660923
H	1.782772	0.532675	-1.025222
C	4.906866	-0.704952	-0.378772
H	5.353015	-2.791272	-0.021513
H	4.134608	1.271712	-0.792833
C	6.314601	-0.258914	-0.253263
C	8.514385	-0.743722	0.088711
C	7.864516	1.410863	-0.264496
C	8.203130	2.852183	-0.398434
C	9.538170	3.284911	-0.291182
C	7.192917	3.803746	-0.633423
C	9.854253	4.638572	-0.416865
H	10.324054	2.551019	-0.109007
C	7.512144	5.156739	-0.757933
H	6.157077	3.472681	-0.716572
C	8.842954	5.578269	-0.650318

H	10.894642	4.962812	-0.332177
H	6.719106	5.886681	-0.939520
C	9.588208	-1.738622	0.347668
C	9.277793	-3.104947	0.482129
C	10.929844	-1.328186	0.460234
C	10.287146	-4.038234	0.723339
H	8.239525	-3.427326	0.395381
C	11.936960	-2.263986	0.701265
H	11.174981	-0.270549	0.356640
C	11.619128	-3.621101	0.833449
H	10.034122	-5.096634	0.825819
H	12.975343	-1.933529	0.786472
C	-0.094053	-1.372834	-0.344087
H	0.011891	-0.412044	0.192018
H	12.408976	-4.353150	1.021809
H	9.091730	6.638369	-0.748162
N	6.581616	1.047844	-0.384404
N	8.859380	0.545108	-0.030146
N	7.254412	-1.183951	-0.014342
N	0.917801	-2.044152	-0.752457
H	-9.382101	-3.130418	-1.135313
H	-6.766108	1.724638	0.319413
H	-6.779295	0.262741	0.941263
O	-8.872324	1.480233	1.603637
H	-9.320195	1.421238	0.745116
H	-8.043471	0.971599	1.445208

Thermal correction to Gibbs Free Energy= 0.5903730 (A.U.)

Electronic Energy= -4195.4368667 (A.U.)

The number of imaginary frequencies: 1

TS_5[Fe-OCHO]*

0 1

C	7.398630	-0.348750	1.368908
N	6.071153	-0.441881	1.191910
C	5.381239	-1.413903	1.844168
C	6.028901	-2.339413	2.671794
C	7.409992	-2.250129	2.839478
C	8.105956	-1.231847	2.181769
Fe	4.969647	0.741312	0.082520
N	3.536001	-0.335116	0.819745
C	2.233443	-0.163738	0.567863
C	1.243231	-1.002794	1.092791

C	1.647870	-2.073431	1.911864
C	2.998634	-2.249421	2.174278
C	3.931169	-1.360632	1.618053
S	4.975269	-0.650509	-1.836291
C	6.419580	-1.600571	-1.912448
N	7.638813	-1.054270	-1.651405
C	8.795172	-1.751866	-1.674165
C	8.807772	-3.093938	-1.989774
C	7.576596	-3.707274	-2.299877
C	6.401780	-2.974199	-2.263243
S	4.667209	2.507722	1.663005
C	3.788228	3.071430	0.268023
N	3.839688	2.162365	-0.741156
C	3.260122	2.414005	-1.923209
C	2.561421	3.593977	-2.161209
C	2.478483	4.539050	-1.124230
C	3.093157	4.285618	0.098368
H	5.440092	-3.440904	-2.480441
H	7.544975	-4.768609	-2.559400
H	9.746075	-3.649198	-2.001735
H	9.694707	-1.181636	-1.432760
H	3.053495	5.005222	0.918487
H	1.935882	5.475986	-1.278040
H	2.095965	3.770531	-3.132358
H	3.366029	1.640766	-2.689124
H	1.967262	0.674205	-0.077963
H	0.899026	-2.747986	2.330481
H	3.334049	-3.069839	2.808773
H	5.458995	-3.115322	3.182943
H	7.933979	-2.963129	3.479680
H	9.186305	-1.118335	2.288044
H	7.902878	0.447301	0.818886
H	7.733279	-0.000209	-1.465661
H	6.255207	1.808810	-0.657237
C	7.218910	2.308878	-1.077023
O	8.153259	1.497386	-1.305259
O	7.138493	3.517365	-1.224082
C	-0.163029	-0.733230	0.773979
H	-0.349346	0.140445	0.123341
N	-1.110261	-1.473709	1.213594
C	-2.449390	-1.164313	0.964389
C	-3.341788	-2.228062	0.718531
C	-2.955319	0.153162	0.997427
C	-4.686515	-1.980344	0.468661

H	-2.953329	-3.248948	0.715580
C	-4.305809	0.393622	0.764784
H	-2.286916	0.984249	1.232741
C	-5.191677	-0.665103	0.487987
H	-5.364027	-2.810022	0.264096
H	-4.688237	1.414472	0.798594
C	-6.627721	-0.401601	0.232218
C	-8.713816	-1.163299	-0.276509
C	-8.362450	1.064047	0.048069
C	-8.883544	2.455208	0.103150
C	-10.247979	2.716386	-0.123359
C	-8.019229	3.530243	0.383491
C	-10.735340	4.023188	-0.070128
H	-10.921722	1.886630	-0.340115
C	-8.509576	4.835920	0.435389
H	-6.961230	3.332352	0.559427
C	-9.868368	5.086487	0.209078
H	-11.796980	4.213757	-0.247121
H	-7.828839	5.662768	0.653607
H	-10.251304	6.109652	0.250496
C	-9.632266	-2.288937	-0.591502
C	-9.152192	-3.611388	-0.634296
C	-10.994346	-2.047410	-0.851552
C	-10.015804	-4.667167	-0.930018
H	-8.097464	-3.802885	-0.433536
C	-11.855370	-3.105361	-1.147215
H	-11.370287	-1.024121	-0.820288
C	-11.369291	-4.417751	-1.187259
H	-9.631751	-5.690040	-0.960236
H	-12.911160	-2.905720	-1.347633
H	-12.044708	-5.245620	-1.418955
N	-7.060620	0.865335	0.288767
N	-9.220325	0.076127	-0.238873
N	-7.424762	-1.442318	-0.046262

Thermal correction to Gibbs Free Energy= 0.5762290 (A.U.)

Electronic Energy= -4307.6487756 (A.U.)

The number of imaginary frequencies: 1

12. Comparisons of catalytic activity

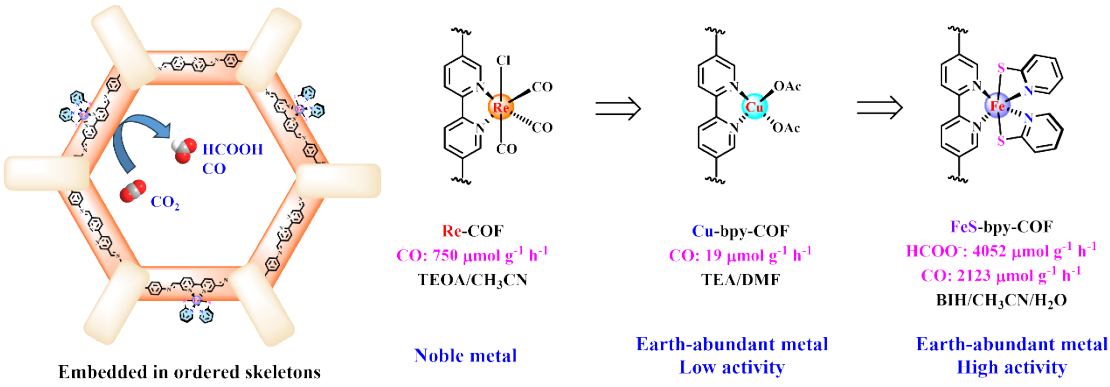

Table S9 Comparison of the performance of Photocatalytic CO_2 conversion with reported photocatalysts.

Catalyst	Photosensitizer Sacrificial agent	Reaction solvent	Product Yield (μmol g^{-1} h^{-1})	TON	Irradiation condition	Ref
Fe-bpy-COF	pySH BIH	CH_3CN/H_2O	4052 ($HCOO^-$) 2123 (CO)	46 4h	λ ≥ 400 nm (300 W Xe lamp)	**This work**
FeS-bpy-COF	BIH	CH_3CN/H_2O	264 ($HCOO^-$) 94 (CO)	3.1 4h	λ ≥ 400 nm (300 W Xe lamp)	**This work**
Re-COF	/ TEOA	CH_3CN	750(CO)	48 20h	λ ≥ 420 nm (225W Xe lamp)	2
Ni-TpBpy	$[Ru(bpy)_3]Cl_2$ TEOA	CH_3CN/H_2O	966(CO)	13.6 5h	λ ≥ 420 nm (300 W Xe lamp)	9
Bpy-sp2c-COF	/ TEOA	CH_3CN	1040(CO)	18.7 17.5h	λ ≥ 420 nm (300 W Xe lamp)	10
COF-367-CoII	/ TEA	CH_3CN	48.6($HCOO^-$) 16.5 (CO) 12.8 (CH_4)	/	λ ≥ 380 nm (300 W Xe lamp)	11
COF-367-CoIII	/ TEA	CH_3CN	93(HCOO-) 5.5 (CO) 10.1 (CH4)	/	λ ≥ 380 nm (300 W Xe lamp)	11
COF-367-Co NSs	$[Ru(bpy)_3]Cl_2$ AA	H_2O	10162 (CO)	20.2 2h	λ ≥ 420 nm (300 W Xe lamp)	12
Co-PI-COF	/ TEOA	CH_3CN	50 (HCOO-)	/	λ ≥ 420 nm (150 W Xe lamp)	13
DQTP COF-Co	$[Ru(bpy)_3]Cl_2$ TEOA	CH_3CN	1020 (CO)	22.5 4h	λ ≥ 420 nm (300 W Xe lamp)	14
Fe SAS/TrCOF	$[Ru(bpy)_3]Cl_2$ TEOA	CH_3CN/H_2O	980.3 (CO)	4.89 4h	λ ≥ 420 nm (300 W Xe lamp)	15
H_2PReBpy-COF	/ TEA	CH_3CN	447 (HCOO-) 1200 (CO)	/	λ ≥ 400 nm (300 W Xe lamp)	16
CoPor-DPP-COF	$[Ru(bpy)_3]Cl_2$ TIPA	CH_3CN/H_2O	10201 (CO)	/	λ ≥ 420 nm (300 W Xe lamp)	17

Co-2,3-DHTA-COF	$[Ru(bpy)_3]Cl_2$ TEOA	CH_3CN/H_2O	18000 (CO)	/	$\lambda \geq 420$ nm (300 W Xe lamp)	18
Cu-Bpy-COF	/ TEA	H_2O	19 (CH_4)	/	$\lambda \geq 420$ nm (300 W Xe lamp)	4
Cu-Bpy-COF	/ TEA	DMF	19 (CO)	/	$\lambda \geq 420$ nm (300 W Xe lamp)	4
Co-TAPT-COF-1	$[Ru(bpy)_3]Cl_2$ TEOA	CH_3CN/H_2O	8390 (CO)	/	$\lambda \geq 420$ nm (300 W Xe lamp)	19
Re-f-COF	/ TEOA	CH_3CN	790 (CO)	/	$\lambda \geq 420$ nm (300 W Xe lamp)	20
Re@TEB-BPY	/ TEA, BNAH	CH_3CN/H_2O	2050 (CH_4)	3.1 12h	$\lambda \geq 400$ nm (300 W Xe lamp)	21
TFBD-COF-Co-SA	$[Ru(bpy)_3]Cl_2$ TEOA	CH_3CN	1480 (CO)	/	$\lambda \geq 420$ nm (300 W Xe lamp)	22
HOF-25-Re	$[Ru(bpy)_3]Cl_2$ TIPA	CH_3CN	3030 (CO)	50.4 2h	$\lambda \geq 420$ nm (300 W Xe lamp)	23
NiPc–CoPOP	$[Ru(bpy)_3]Cl_2$ TEOA	CH_3CN/H_2O	1942 (CO)	/	$\lambda \geq 400$ nm (White LED)	24

13. References

1. Y. K. Zhang, L. Zhao, W. J. Xie, H. R. Li and L. N. He, *ChemSusChem*, 2024, **17**, e202400090.
2. S. Yang, W. Hu, X. Zhang, P. He, B. Pattengale, C. Liu, M. Cendejas, I. Hermans, X. Zhang, J. Zhang and J. Huang, *J. Am. Chem. Soc.*, 2018, **140**, 14614-14618.
3. M. Khrizanforov, S. Strekalova, V. Khrizanforova, V. Grinenko, K. Kholin, M. Kadirov, T. Burganov, A. Gubaidullin, T. Gryaznova, O. Sinyashin, L. Xu, D. A. Vicic and Y. Budnikova, *Dalton Trans*, 2015, **44**, 19674-19681.
4. Y. Zhang, L. Cao, G. Bai and X. Lan, *Small*, 2023, **19**, 2300035.
5. F. Weigend and R. Ahlrichs, *Phys. Chem. Chem. Phys.*, 2005, **7**, 3297-3305.
6. Z. Liu, T. Lu and Q. Chen, *Carbon*, 2020, **165**, 461-467.
7. M. J. Frisch, G. W. Trucks, H. B. Schlegel, G. E. Scuseria, M. A. Robb, J. R. Cheeseman, G. Scalmani, V. Barone, G. A. Petersson, H. Nakatsuji, X. Li, M. Caricato, A. V. Marenich, J. Bloino, B. G. Janesko, R. Gomperts, B. Mennucci, H. P. Hratchian, J. V. Ortiz, A. F. Izmaylov, J. L. Sonnenberg, Williams, F. Ding, F. Lipparini, F. Egidi, J. Goings, B. Peng, A. Petrone, T. Henderson, D. Ranasinghe, V. G. Zakrzewski, J. Gao, N. Rega, G. Zheng, W. Liang, M. Hada, M. Ehara, K. Toyota, R. Fukuda, J. Hasegawa, M. Ishida, T. Nakajima, Y. Honda, O. Kitao, H. Nakai, T. Vreven, K. Throssell, J. A. Montgomery Jr., J. E. Peralta, F. Ogliaro, M. J. Bearpark, J. J. Heyd, E. N. Brothers, K. N. Kudin, V. N. Staroverov, T. A. Keith, R. Kobayashi, J. Normand, K. Raghavachari, A. P. Rendell, J. C. Burant, S. S. Iyengar, J. Tomasi, M. Cossi, J. M. Millam, M. Klene, C. Adamo, R. Cammi, J. W. Ochterski, R. L. Martin, K. Morokuma, O. Farkas, J. B. Foresman and D. J. Fox, *Journal*, 2016.
8. H. J. Kuhn, S. E. Braslavsky and R. Schmidt, *Pure Appl. Chem.*, 2004, **76**, 2105-2146.
9. W. Zhong, R. Sa, L. Li, Y. He, L. Li, J. Bi, Z. Zhuang, Y. Yu and Z. Zou, *J. Am. Chem. Soc.*, 2019, **141**, 7615-7621.

10. Z. Fu, X. Wang, A. M. Gardner, X. Wang, S. Y. Chong, G. Neri, A. J. Cowan, L. Liu, X. Li, A. Vogel, R. Clowes, M. Bilton, L. Chen, R. S. Sprick and A. I. Cooper, *Chem. Sci.*, 2020, **11**, 543-550.
11. Y. N. Gong, W. Zhong, Y. Li, Y. Qiu, L. Zheng, J. Jiang and H. L. Jiang, *J. Am. Chem. Soc.*, 2020, **142**, 16723-16731.
12. W. Liu, X. Li, C. Wang, H. Pan, W. Liu, K. Wang, Q. Zeng, R. Wang and J. Jiang, *J. Am. Chem. Soc.*, 2019, **141**, 17431-17440.
13. T. Skorjanc, D. Shetty, M. E. Mahmoud, F. Gándara, J. I. Martinez, A. K. Mohammed, S. Boutros, A. Merhi, E. O. Shehayeb, C. A. Sharabati, P. Damacet, J. Raya, S. Gardonio, M. Hmadeh, B. R. Kaafarani and A. Trabolsi, *ACS Appl. Mater. Interfaces*, 2021, **14**, 2015-2022.
14. M. Lu, Q. Li, J. Liu, F.-M. Zhang, L. Zhang, J.-L. Wang, Z.-H. Kang and Y.-Q. Lan, *Appl. Catal., B*, 2019, **254**, 624-633.
15. L. Ran, Z. Li, B. Ran, J. Cao, Y. Zhao, T. Shao, Y. Song, M. K. H. Leung, L. Sun and J. Hou, *J. Am. Chem. Soc.*, 2022, **144**, 17097-17109.
16. D. Song, W. Xu, J. Li, J. Zhao, Q. Shi, F. Li, X. Sun and N. Wang, *Chin. J. Catal.*, 2022, **43**, 2425-2433.
17. X. Wang, X. Ding, T. Wang, K. Wang, Y. Jin, Y. Han, P. Zhang, N. Li, H. Wang and J. Jiang, *ACS Appl. Mater. Interfaces*, 2022, **14**, 41122-41130.
18. Q. Zhang, S. Gao, Y. Guo, H. Wang, J. Wei, X. Su, H. Zhang, Z. Liu and J. Wang, *Nat. Commun.*, 2023, **14**, 1147.
19. W. Zhou, X. Wang, W. Zhao, N. Lu, D. Cong, Z. Li, P. Han, G. Ren, L. Sun, C. Liu and W.-Q. Deng, *Nat. Commun.*, 2023, **14**, 6971.
20. D. H. Streater, E. R. Kennehan, D. Wang, C. Fiankor, L. Chen, C. Yang, B. Li, D. Liu, F. Ibrahim, I. Hermans, K. L. Kohlstedt, L. Luo, J. Zhang and J. Huang, *J. Am. Chem. Soc.*, 2024, **146**, 4489-4499.
21. F. A. Rahimi, S. Dey, P. Verma and T. K. Maji, *ACS Catal.*, 2023, **13**, 5969-5978.
22. Y. Yang, Y. Lu, H.-Y. Zhang, Y. Wang, H.-L. Tang, X.-J. Sun, G. Zhang and F.-M. Zhang, *ACS Sustainable Chem. Eng.*, 2021, **9**, 13376-13384.
23. B. Yu, L. Li, S. Liu, H. Wang, H. Liu, C. Lin, C. Liu, H. Wu, W. Zhou, X. Li, T. Wang, B. Chen and J. Jiang, *Angew. Chem. Int. Ed.*, 2021, **60**, 8983-8989.
24. X. Y. Dong, Y. N. Si, Q. Y. Wang, S. Wang and S. Q. Zang, *Adv. Mater.*, 2021, **33**, 2101568.